Journal of Photochemistry and Photobiology B: Biology 148 (2015) 128–135

Contents lists available at ScienceDirect

Journal of Photochemistry and Photobiology B: Biology

journal homepage: www.elsevier.com/locate/jphotobiol

Combined experimental and computational investigation of the absorption spectra of *E*- and *Z*-cinnamic acids in solution: The peculiarity of *Z*-cinnamics

María L. Salum [a], Pau Arroyo Mañez [b], F. Javier Luque [c], Rosa Erra-Balsells [a,*]

[a] CIHIDECAR-Departamento de Química Orgánica, FCEN, Universidad de Buenos Aires, Pabellón II, 3er P, Ciudad Universitaria, 1428 Buenos Aires, Argentina
[b] Departamento de Química Orgánica and UMYMFOR (CONICET-UBA), FCEN, Universidad de Buenos Aires, Pabellón II, 3er P, Ciudad Universitaria, 1428 Buenos Aires, Argentina
[c] Departament de Fisicoquímica, Facultat de Farmacia and Institut de Biomedicina (IBUB), Universitat de Barcelona, E-08028 Barcelona, Spain

ARTICLE INFO

Article history:
Received 25 September 2014
Received in revised form 23 March 2015
Accepted 28 March 2015
Available online 13 April 2015

ABSTRACT

Cinnamic acids are present in all kinds of plant tissues and hence in herbs and derived medicines, cosmetics and foods. The interest in their role in plants and their therapeutic applications has grown exponentially. Because of their molecular structure they can exist in *E*- and *Z*-forms, which are both found in plants. However, since only the *E*-forms are commercially available, very few *in vitro* and *in vivo* studies of the *Z*-form have been reported. In this work the physico-chemical properties of *Z*-cinnamic acids in solution have been examined by means of UV-absorption spectroscopy and high-level quantum mechanical computations. For each isomer similar absorption spectra were obtained in methanol and acetonitrile. However, distinct trends were found for *Z*- and *E* forms of cinnamic acids in water, where a higher hypsochromic shift of the *Z*-isomer relative to the *E*-form was observed. In general the wavelength of maximal absorption of the *Z*-form is dramatically blue shifted (−30 to −40 nm) to $\lambda < 280$ nm, while a slightly blue shift of the absorption maxima for the corresponding *E*-form (+3 to −4 nm) was observed. This difference is associated with the non-planar, largely distorted, *Z*-structure and to the almost complete flat structure of the *E*-form. The results provide a basis for the study of functional and biotechnological roles of cinnamic acids and for the analysis of samples containing mixture of both geometric isomers.

© 2015 Published by Elsevier B.V.

1. Introduction

Cinnamic acids (phenylpropenoic acids; cinnamics) belong to the family of plant growth regulators together with zeatin, abscisic acid and jasmonic acid [1]. Because of their molecular structure they can exist in both *E*- and *Z*-forms (Scheme 1), which are both found in plants [1,2]. *Z*/*E*-isomers of coumaric acid, caffeic acid and ferulic acid have been detected in a number of dicots and monocots [3,4]. They play important roles in plant growth and in plant-environment interactions and also function as cell wall components, anti-herbivory compounds, UV protectants, pigments and aroma compounds [5,6]. Furthermore, derivatives of cinnamic acids have been reported to have antibacterial, antiviral and antifungal properties [7].

In nature the important intermediate of the phenylpropenoid pathway, *E*-cinnamic acid (*E*-3-phenylpropenoic acid, *E*-CA), is synthesized from *L*-phenylalanine by phenylalanine ammonia lyase and then converted by enzymatic reactions to other metabolites, such as *E*-coumaric acid (*E*-4-hydroxy-cinnamic acid), *E*-ferulic acid (*E*-3-methoxy-4-hydroxy-cinnamic acid), *E*-caffeic acid (*E*-3,4-dihydroxy-cinnamic acid) and *E*-sinapinic acid (*E*-3,5-dimethoxy-4-hydroxy-cinnamic acid) [1,2,8]. In contrast, the origin of *Z*-cinnamics is still under discussion. Their presence in root tissue suggests that they may be produced through both light-dependent and light-independent pathways or may be transported from a plant organ to another [9]. Some authors suggested that they might be UV light-mediated photoisomerization products of *E*-cinnamics [10] because their concentration is enhanced by UV irradiation. Given the fact that *Z*-isoforms of coumaric and ferulic acids were detected in plants after UV or sunlight irradiation [8], *Z*-cinnamics in plants grown in open fields are believed to reachμM levels in plant tissues. As a matter of fact, the exact percentage of *Z*-cinnamics present as free acids and conjugates in plant cell is still unknown [11].

The biological properties of *Z*-cinnamics are distinctly different from those of *E*-cinnamics. Thus, *E*-cinnamic acid is used as a precursor for the biosynthesis of numerous phenolic compounds such as flavonoids, phytoalexin, salicylic acid and lignin [10]. It has also been related to stiffening of the cell wall and reduction in root

* Corresponding author.
E-mail address: erra@qo.fcen.uba.ar (R. Erra-Balsells).

http://dx.doi.org/10.1016/j.jphotobiol.2015.03.032
1011-1344/© 2015 Published by Elsevier B.V.

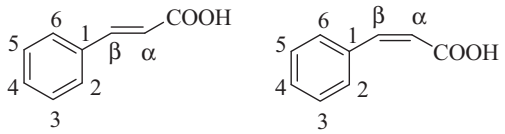

Scheme 1. Chemical structure and numbering of *E*- and *Z*-cinnamic acids.

growth [12]. In contrast, *Z*-cinnamic acid has been shown to have cell elongation-promoting activities and to inhibit gravitropic response, in addition to its role in seed germination and in delaying the ethylene surge [10]. Guo et al. [11] have also provided some insights into the molecular mechanisms by which *Z*-cinnamics regulate plant growth and development as well as plant adaptation to environmental stresses.

Taking advantage of the highly efficient one-pot preparation of *Z*-cinnamic acids by *E*–*Z* photoisomerization developed in our group [13,14], we decided to study their UV absorption properties in different solvents (methanol, acetonitrile and in aqueous solution) and compare their spectral properties with those of the corresponding *E*-isomer. Further, we also examined the influence of pH on the spectral properties in aqueous solution. Finally, high-level quantum mechanical computations were used as a tool to rationalize the experimental results. Overall, the study provides a detailed description of the spectral properties of *Z*-cinnamic acids, which should be valuable to assist the functional and biotechnological roles of these compounds.

2. Experimental

2.1. Material and reagents

E-cinnamic acid (*E*-CA), *E*-4-hydroxycinnamic acid (*E*-coumaric acid, *E*-CUA), *E*-3-methoxy-4-hydroxycinnamic acid (*E*-ferulic acid, *E*-FA), *E*-3,5-dimethoxy-4-hydroxycinnamic acid (*E*-sinapinic acid, *E*-SA), *E*-3,4-dioxymethylencinnamic acid (*E*-DMCA), *E*-3,4-dihydroxycinnamic acid (caffeic acid, *E*-CAFA), *E*-3-hydroxy-4-methoxycinnamic acid (isomer ferulic acid, *E*-IFA), *E*-3-chloro-4-methoxycinnamic acid (*E*-3C4MCA), *E*-2-hydroxycinnamic acid (*E*-2HCA), *E*-3-hydroxycinnamic acid (*E*-3HCA), *E*-4-nitrocinnamic acid (*E*-4NOCA), *E*-4-aminocinnamic acid hydrochloride (*E*-4ACA), 3-(*E*-3,4-dihydroxycinnamoyl)quinic acid (chlorogenic acid, 3-caffeoylquinic acid, *E*-3-CAFQA), aliphatic organic amines (ethanolamine, butylamine, pyperidine) and cysteamine hydrochloride were purchased from Aldrich Chemical Co. All the solvents (Sigma–Aldrich HPLC grade) were used as purchased without further purification. Water of very low conductivity (Milli-Q grade) was used. *Z*-cinnamic acid (*Z*-cinnamic acid, *Z*-CA), *Z*-4-hydroxycinnamic acid (*Z*-coumaric acid, *Z*-CUA), *Z*-3-methoxy-4-hydroxycinnamic acid (*Z*-ferulic acid, *Z*-FA), *Z*-3,5-dimethoxy-4-hydroxycinnamic acid (*Z*-sinapinic acid, *Z*-SA,) were synthesized by photoisomerization of the corresponding *E*-cinnamic acid in acetonitrile solution as was described elsewhere [13]. Briefly, the ionic liquid ammonium *E*-cinnamate prepared with an *E*-cinnamic acid and an aliphatic organic amine (i.e., butylamine or ethanolamine) was irradiated in acetonitrile solution. From the precipitated solid ionic liquid *Z*-cinnamic acid (IL Z-CH.Am) the corresponding free *Z*-cinnamic acid was obtained as follows: the IL *Z*-CH.Am, was dissolved in water and (i) passed through an ion-exchange column chromatography (Sigma–Aldrich Dowex 50WX8-200 ion-exchange resin) and water removed by evaporation under vacuum (freeze-drying) or (ii) just after adjusting the pH of the water solution with HCl, extracting twice with CH_2Cl_2 and then removing the solvent by evaporation under vacuum. Then, they were fully characterized (m.p., ^{1}H and ^{13}C NMR, UV–vis absorption spectroscopy) by comparison with the authentic sample previously described [13].

2.2. UV–visible absorption spectroscopy

UV–visible absorption spectra of the cinnamic acids methanolic solutions were recorded on a Shimadzu UV-1203 spectrophotometer. Measurements were made in quartz cells of 1 cm optical-path length (Hellma, Germany).

2.3. Effect of adding water to methanolic solution

Mixtures of methanol–water were prepared in the range 2.95:0.05–0.20:2.80 MeOH:H_2O v/v. *E*- and *Z*-cinnamic acids concentration range was $2.5–4.3 \cdot 10^{-5}$ M.

2.4. Effect of adding organic aliphatic base to methanolic solution

A stock solution of the amine at $6.5 \cdot 10^{-4}$ M in methanol was prepared. Mixtures of methanol–methanol amine solution (MeOH–A.MeOH) were prepared in the range 2.99:0.01–0.20:2.80 MeOH:A.MeOH v/v. *E*- and *Z*-cinnamic acids concentration range was $2.5–4.3 \cdot 10^{-5}$ M.

2.5. Effect of adding organic aliphatic base to acetonitrile solution

A stock solution of the amine at $6.5 \cdot 10^{-4}$ M in acetonitrile was prepared. Mixtures of acetonitrile–acetonitrile amine solution (MeCN–A.MeCN.) were prepared in the range 2.99:0.01–0.20:2.80 MeCN:A.MeCN v/v. *E*- and *Z*-cinnamic acids concentration range was $2.5–4.3 \cdot 10^{-5}$ M.

3. Computational details

All ground state structures of neutral and anionic species were optimized at the MP2 level of theory together with the 6-311++G(d,p) basis set. Optimizations were carried out using the Berny analytical gradient optimization method [15,16]. Stationary points were characterized by analysis of vibrational frequencies, which were all positives. Vertical energies of the excited states were calculated using the TDDFT method for the optimized structures of the ground state using the PBE0 [17] functional together with the basis sets 6-311++G(2d,2p) and aug-cc-dVDZ [18], and the B3LYP/6-31G(d) level of theory.

In the geometry optimizations up to four explicit water molecules were considered in order to account for structural effects due to hydration of the *Z*- and *E*-sinapinic acid. Solvent effects in TD–PBE calculations were considered using a self-consistent reaction field (SCRF) [19] based on the integral equation formalism of the polarizable continuum model (PCM) [20,21]. All calculations were carried out with the Gaussian03 suite of programs [22].

4. Results

The effect of solvation in acetonitrile, methanol and water on the UV absorption spectra of *Z*- and *E*-3,5-dimethoxy-4-hydroxycinnamic acid (sinapinic acid, SA; *Z*-SA and *E*-SA) is shown in Fig. 1. The *E*-form of SA shows single absorption bands between 321 and 313 nm in acetonitrile (321 nm), methanol (317 nm) and water (313 nm). Thus, on moving from acetonitrile to methanol to water a minor hypsochromic shift was observed. Unexpectedly, a notorious hypsochromic shift was found for the absorption spectra of *Z*-SA in these solvents, as the single band at maximum wavelength was in the range 319–280 nm (319 nm in acetonitrile and 280 nm in water). The combination of all the spectra described above in a

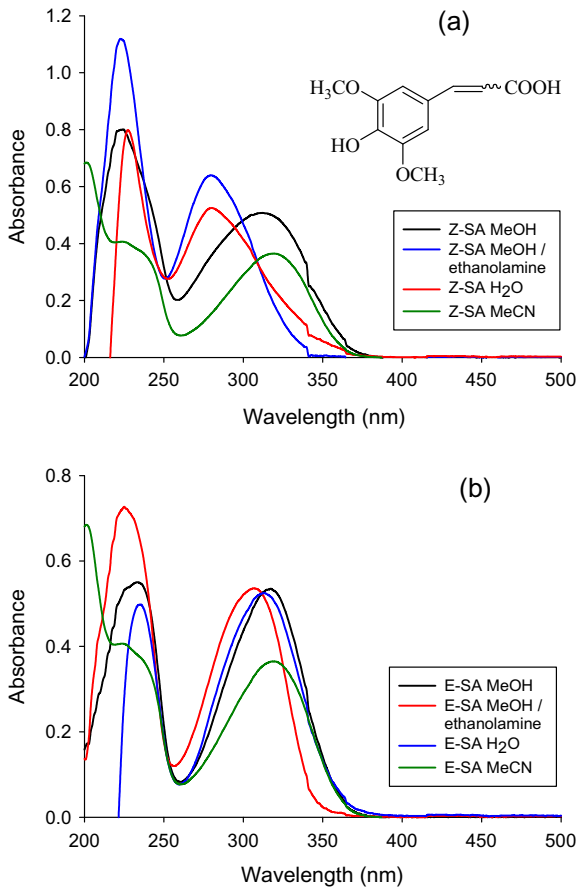

Fig. 1. Effect of solvent on the UV absorption spectra of *Z*- and *E*-SA. (a) *Z*-SA ($4.4 \cdot 10^{-5}$ M): — MeCN, — MeOH, —— H_2O, —— MeOH + ethanolamine; (b) *E*-SA ($2.8 \cdot 10^{-5}$ M): — MeCN, — MeOH, —— H_2O, —— MeOH + ethanolamine. MeOH + ethanolamine (ethanolamine $6.2 \cdot 10^{-4}$ M in MeOH).

single comparative figure is included in Supplementary material (Fig. S1).

Similar differential solvent-induced shifts in the absorption maxima were observed in the UV spectra of *Z*- and *E*-4-hydroxycinnamic acid (coumaric acid, CUA, *Z*- and *E*-CUA), *Z*- and *E*-4-hydroxy-3-methoxycinnamic acid (ferulic acid, FA, *Z*- and *E*-FA) and *Z*- and *E*-3,4-dioxymethylencinnamic acid (DMCA, *Z*- and *E*-DMCA) (Table 1; see also Figs. S2–S4 in Supplementary Material). This finding suggests that the intramolecular interaction between the methoxy and hydroxy groups present in the cinnamic acid derivatives has only a moderate influence on the propenoic fragment, in agreement with previous experimental and theoretical studies conducted on *E*-cinnamics [23,24]. Nevertheless, a small effect was found in the case of cinnamic acid (CA), since for *Z*-CA the band shift was much lower relative to the other compounds (from 261 nm in MeCN to 254 nm in H_2O; see Table 1 and Fig. S5). The absence of a polar substituent in the cinnamic moiety would be the cause of the minor effect observed for this compound.

4.1. Effect of added organic bases and water

The important hypsochromic shifts observed in water solution encouraged us to study the effect of adding an organic aliphatic base such as ethanolamine to the methanol solution. This idea was based on our previous experience with ionic liquids (ILs) prepared with cinnamic acids and ethanolamine (Am), among other aliphatic amines [13]. As described elsewhere [13], the UV absorption spectrum of the IL *E*-SA.Am (1:1; mol/mol) in MeOH showed a single band located at 307 nm, and that of the IL *Z*-SA.Am (1:1; mol/mol) a single band at 280 nm (Table 1). When the acid to amine ratio was increased (i.e., acid/amine mol/mol: 1:2. 1:3, 1:5, 1:10 and so on), the spectra of the *E*-SA + Am mixtures in MeOH were quite similar among them and similar to that of the *E*-SA + Am 1:1 in the same solvent. However, a larger hypsochromic shift was found in the spectra of the *Z*-SA + Am series, which resembled the profile found for the *Z*-SA + Am mixture with 1:1 M ratio. As an example, Fig. 1(a) and (b) shows the spectra obtained for *Z*- and *E*-SA, respectively, in the presence of ethanolamine $6.4 \cdot 10^{-4}$ M in methanol, for a SA: ethanolamine ratio of 1:10 (mol:mol). It can be seen that the band shifted from 317 nm (MeOH) to 307 nm for *E*-SA, and from 312 nm (MeOH) to 280 nm for *Z*-SA, the latter matching the value observed for the *Z*-isomer in water solution (Table 1; see also Fig. S1 for the combined representation of the *E*-SA and *Z*-SA spectra).

Fig. 2(a) and (b) shows the effect triggered by the addition of different organic bases (ethanolamine; butylamine; pyperidine) to the methanolic solution of *Z*-FA ($4.3 \cdot 10^{-5}$ M; solution volume, 3 mL). The results obtained by adding increasing volumes (mL) of a MeOH solution ($6.5 \cdot 10^{-4}$ M) of the amines showed that addition of up to 0.5 mL leads to a significant reduction in the absorbance at

Table 1
UV absorption spectra of *E*- and *Z*-cinnamic acids and their cinnamates in methanol, water and acetonitrile solution.

Acid	Solvent	λ_{max} (nm)			
		E-acid	*Z*-acid	*E*-acid + Am[a]	*Z*-acid + Am[a]
CA	MeCN	268	261	273	–
	MeOH	268 (4.12)	257.5	266	258
	H_2O	271 (4.20)	254	269	258
CUA	MeCN	298	298.5	300	–
	MeOH	289 (4.16)	297	286	268
	H_2O	286.5 (4.05)	267	285	265
FA	MeCN	319, 295sh	317, 296sh	319	–
	MeOH	316 (4.02), 289sh	316.5	313	268, 297sh
	H_2O	312 (4.01), 289sh	268, 298sh	310	267, 298sh
SA	MeCN	321 (4.09)	319	322	–
	MeOH	317 (4.01)	312	307	280
	H_2O	313	280	302	278
DMCA	MeCN	324	320	319, 293sh	–
	MeOH	319.5 (3.98)	312, 273sh	318	304
	H_2O	320 (3.90)	270, 305sh	316	305

[a] Acid + Am, cinnamate prepared with ethanolamine (Am); molar ratio cinnamic acid: ethanolamine 1:1 (mol/mol).

316 nm and an increase in the absorbance at 269 nm. Further, the obtained absorbance values are mostly unaltered by extra addition of the amine solution.

The effect of adding successively increasing amounts of water to the methanolic solution of cinnamic acids was also explored. As an example, the effect of adding increasing amounts of water to the MeOH solution of *Z*- and *E*-FA is shown in Fig. 3(a) and (b), respectively. The change in the structure of the *Z*-FA chromophore is clearly observed in Fig. 3(a), in a similar way to what occurred by addition of the organic bases. Thus, in methanol the neutral species, with a single absorption band at aprox. 317 nm is still the predominant form till addition of 1 mL of water (methanol:water 2:1 v/v). From this point a shoulder around 270 nm was detected and becomes the predominant band with a maximum at 269 nm and a shoulder at 298 when 2.80 mL of water was added (methanol:water 0.20:2.80 v/v); thus, the mono anionic form (carboxylate anion) would be present in the solution. Similar experiments conducted with the methanolic solution of *E*-FA indicated that the degree of conjugation in the cinnamic acid moiety is almost unaltered by the presence of water in the environment (Fig. 3(b)), as only a minor blue shift in the predominant band (316-313 nm) was observed (Table 1).

The preceding experiments reveal a qualitatively similar pattern in the absorbance changes triggered upon addition of water and organic bases to the methanolic solutions, although the rate of the absorbance shift recorded at 316 and 269 nm and the final absorbance values are slightly different for water and the aliphatic amines. Furthermore, these values and the corresponding final spectra matched the spectrum obtained in water solution. Overall, the results point out that in these experiments a new cinnamic acid-like absorbing species (i.e., the mono anionic carboxylate form) is produced and stabilized by solvation with water molecules and by the amine in methanolic solutions. Hence, it is not surprising that when the amine was added as hydrochloride (i.e., cysteine hydrochloride) the spectra was practically not affected, within the experimental error. In these conditions the anion carboxylate is not formed because the basic character of the nitrogen is lost (Fig. 2(a) and (b)).

The addition of water to acetonitrile solutions showed again a small effect on the absorption spectra of *E*-FA and a large hypsochromic shift for *Z*-FA, as illustrated in Fig. 2(a) and (b), which reveal a large resemblance with the absorbance shifts obtained upon addition of water to methanolic solutions. The effect of adding organic bases on the absorbance spectra in acetonitrile solutions is however less pronounced compared to the MeOH solutions, as can be noted in Figs. S6 and S7 in Supplementary Material. Thus, compared to the methanolic solutions, addition of the organic base to CH_3CN solutions leads to a minor increase of the band absorption at 269 nm and a minor decrease at 316 nm. As described elsewhere [13], this difference can be attributed to the very low solubility of the IL of *Z*-cinnamic acids (cinnamate anions, carboxylate anions in general) in acetonitrile, because of the aprotic character of the solvent. Thus, only very minor amount of carboxylate-like species would be present in the media. Similarly, the addition of increasing amounts of water to solutions of *E*-FA in methanol and acetonitrile led to a very minor decrease of the band at 316 nm (ΔAbs < 0.06 u.a.) and increase at 269 nm (ΔAbs < 0.08 u.a.) (see Figs. S6 and S7 in Supplementary Material).

As a final remark, comparison of the dependence of absorbance band intensity in the methanolic solution of cinnamic acids on the

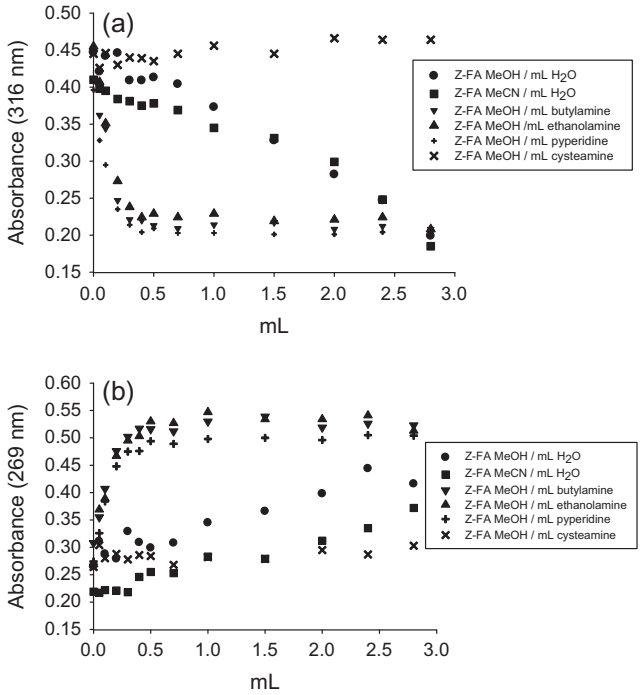

Fig. 2. Effect of adding water and organic bases to methanolic and acetonitrile solutions of *Z*-FA. *Z*-FA in methanol ($4.3 \cdot 10^{-5}$ M): ● H_2O, ▲ ethanolamine, ▼ butylamine; + pyperidine; **x** cysteine hydrochloride. *Z*-FA in acetonitrile ($4.3 \cdot 10^{-5}$ M): ■ H_2O. Monitoring wavelength, (a) 316 nm and (b) 269 nm. Organic bases are added as methanolic solution ($6.5 \cdot 10^{-4}$ M) to *Z*-FA in MeOH.

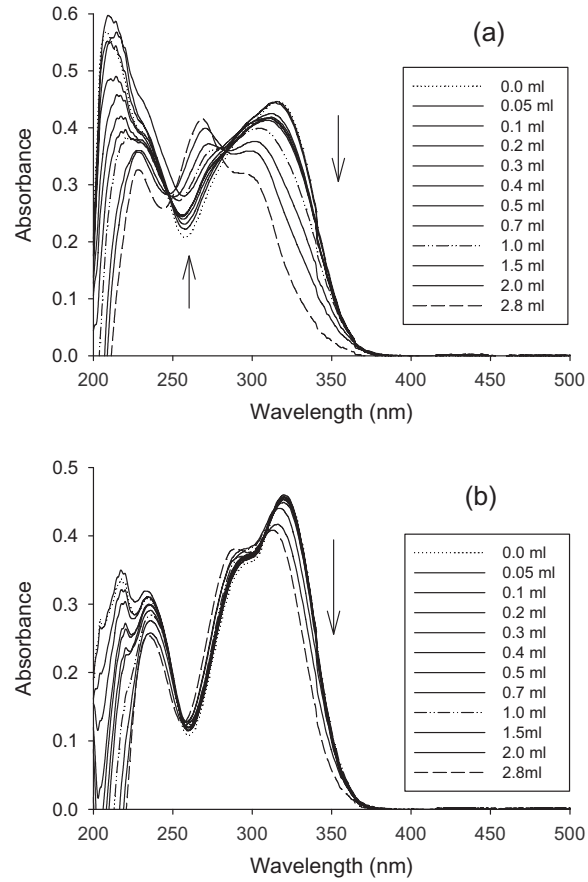

Fig. 3. Effect of adding water to the methanolic solution on the UV absorption spectra of (a) *Z*-FA and (b) *E*-FA (4.3 and $2.5 \cdot 10^{-5}$ M in methanol, respectively); mL of H_2O added are indicated in the inset; solution volume, 3 mL.

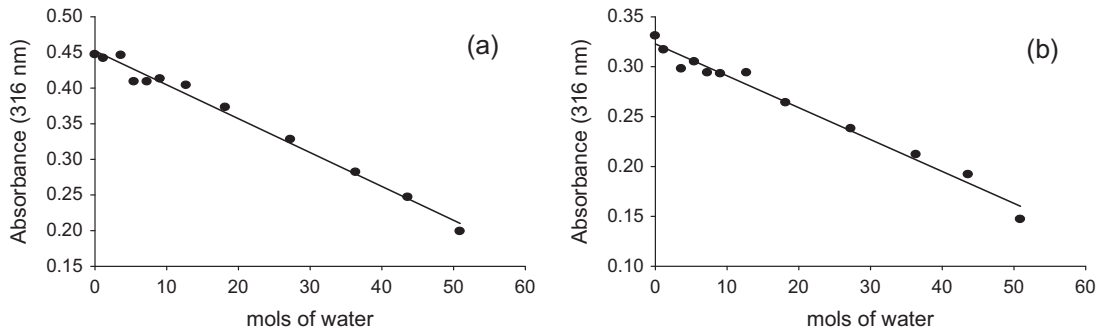

Fig. 4. Dependence of the absorbance of the band at 316 nm on the moles of water added to the methanolic solution of (a) *Z*-FA ($1.03 \cdot 10^{-7}$ M), $y = 0.4452–0.0047x$ and (b) *Z*-SA ($1.07 \cdot 10^{-7}$ M), $y = 0.3229–0.0032x$. Volume of all the solutions = 3 mL; MeOH volume in each solution (from 0 to 50.91 mols of water): 3.0, 2.9, 2.8, 2.7, 2.6, 2.5, 2.3, 2.0, 1.5, 1.0, 0.6 and 0.2 mL.

amount of added water is shown in Fig. 4(a) and (b) for *Z*-FA and *Z*-SA, respectively. The results reveal a similar dependence for the two compounds, suggesting the involvement of similar chromophoric species (neutral carboxylic form and anionic carboxylate form).

4.2. Effect of pH in water solution

The effect of pH on the absorption spectra of *E*- and *Z*-SA water solutions was determined by adding sodium hydroxide or hydrochloric acid. Thus, on diminishing the pH of the water solution for *E*-SA, the original single band at 313 nm was bathochromically shifted to 317 nm, matching with the band observed in methanol (Fig. 5(c)), which would correspond to the protonated species. In water solution, a base such as sodium hydroxide was required to generate a new absorption band, red shifted to 370 nm, attributable to the extended conjugation between the carboxylic unit and the phenoxy group at C4 in the dianionic form of *E*-SA (Fig. 5(d)), as expected from the reported ionization constants for *E*-sinapinic acid ($pK_{a1} \sim 4.3$; $pK_{a2} \sim 9.2$ [25]). For *Z*-SA (Fig. 5(a)) on diminishing the pH of the water solution, the original single band at 280 nm was bathochromically

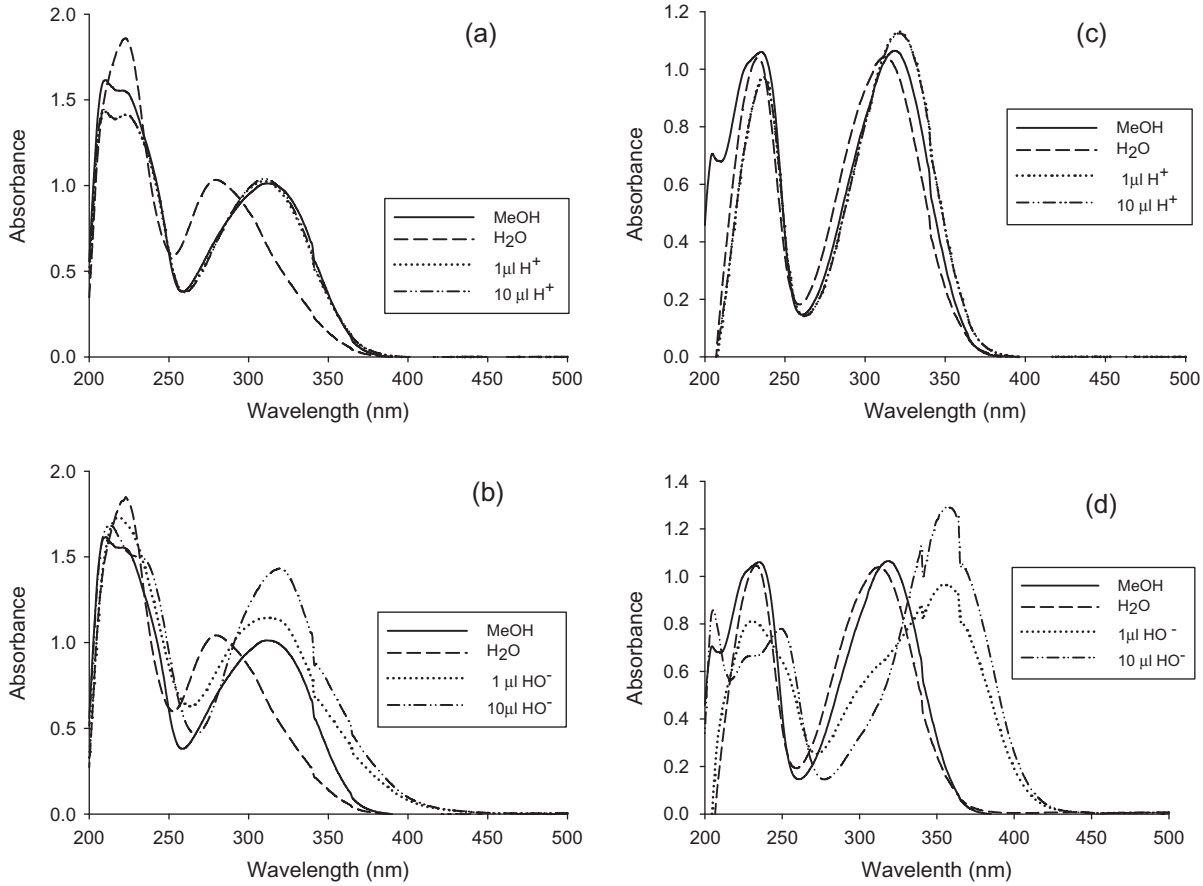

Fig. 5. UV absorption spectra of (a and b) *Z*-SA ($1.1 \cdot 10^{-4}$ M) in methanol (—), water (- - -) and the effect of adding (a) HCl (1 M) in the water solution, 1 µL (···) and 10 µL (-·-·-); (b) NaOH (1 M) to the water solution, 1 µL (···) and 10 µL (-·-·-); (c and d) *E*-SA ($6.5 \cdot 10^{-5}$ M) in methanol (—), water (- - -) and the effect of adding (d) HCl (1 M) to the water solution, 1 µL (···) and 10 µL (-·-·-); (d) NaOH (1 M) to the water solution, 1 µL (···) and 10 µL (-·-·-).

Table 2
Side chain dihedral angles of the neutral, mono (carboxylate) and di (carboxylate and phenolate) anionic *Z*- and *E*-SA geometries optimized in vacuum and in presence of water molecules at the MP2/6-311++G(d,p) level. Absorption wavelength (λ_{max}; nm) computed for the excited states from TD-PBE0 calculations.

System	Dihedral angles		λ_{max} [d]	λ_{max} [e]
	C2=C1—Cβ=Cα[a]	O=C—Cα=Cβ		
Z-SA	45	20[b]	343/343/344	312
Z-SA + H_2O	45	65[b]	292/292/292	
Z-SA + $2H_2O$	44	41[b]	324/324/325	
Z-SA + $3H_2O$	37	56[b]	308/307/307	
Z-SA$^-$	35	77[b]	284/284/299	280
Z-SA$^-$ + H_2O	20	111[b]	285/285/297	
Z-SA$^-$ + $2H_2O$	32	59[b]	287/288/308	
Z-SA$^-$ + $3H_2O$	41	97[b]	275/276/288	
Z-SA^{2-}	8	−31[b]	357/357/347	350
Z-SA^{2-} + H_2O	1	−31[b]	354/ 354/345	
Z-SA^{2-} + $2H_2O$	−4	−58[b]	346/347/334	
Z-SA^{2-} + $3H_2O$	−1	−51[b]	350/351/339	
E-SA	0	180[c]	339/340/339	317
E-SA + H_2O	18	176[c]	338/338/337	
E-SA + $2H_2O$	18	179[c]	336/336/336	
E-SA + $3H_2O$	13	176[c]	337/337/336	
E-SA$^-$	25	−170[c]	298/299/286	313
E-SA$^-$ + H_2O	25	−168[c]	300/301/287	
E-SA$^-$ + $2H_2O$	22	−167[c]	296/297/289	
E-SA$^-$ + $3H_2O$	23	−179[c]	301/301/290	
E-SA^{2-}	−12	−175[c]	364/365/348	370
E-SA^{2-} + H_2O	−10	−176[c]	368/368/350	
E-SA^{2-} + $2H_2O$	−4	178[c]	370/371/352	
E-SA^{2-} + $3H_2O$	−3	176[c]	371/372/353	
E-SA^{2-} + $4H_2O$	−2	175[c]	370/371/352	

[a] Considering the *S*-cis configuration of the double bonds involved.
[b] Considering the *S*-cis configuration of the double bonds involved obtained from the geometrical optimization of the neutral *Z*-SA.
[c] Considering the *S*-trans configuration of the double bonds involved obtained from the geometrical optimization of the neutral *E*-SA.
[d] Values determined at the TD-PBE0 level with (left) 6-311++(2d2p) and (center) aug-cc-pVDZ basis, and (right) the B3LYP/6-31G(d) level and basis set.
[e] Experimental values.

shifted to 312 nm, matching with the band observed in methanol. However, on increasing the pH, in contrast with *E*-SA, the band of *Z*-SA was red shifted to 312 nm (Fig. 5(b)), which is similar to the typical band observed in methanol solution (λ_{max} 312 nm). Extra amount of aqueous sodium hydroxide solution added did not modify the spectrum. The above mentioned extended conjugation between the carboxylic unit and the phenoxy group at C4 in the dianionic form of Z-SA would not take place because of its large deviation from planarity.

4.3. Theoretical calculations of electronic transitions

Quantum chemical calculations have become a standard approach valuable for the assignment of the experimental spectra and to get insights into the underlying optical and electronic properties. In particular, time-dependent DFT (TDDFT) [26] calculations have proved to be well suited for predicting the spectral properties of cinnamic acid derivatives [27,28]. In this work, the absorption properties of the *Z*- and *E*-SA have been investigated by means of TDDFT computations and solvent effects have been accounted for by using the IEF-PCM solvation continuum model. Table 2 reports selected conformational parameters of *Z*- and *E*-SA taken from the molecular geometries optimized at the MP2/6-311++G(d,p) level and the predicted wavelengths for electronic transitions determined from TDDFT–PBE0 calculations using two different basis sets (6-311++(2d2p) and aug-cc-pVDZ), in comparison with the results obtained with a less accurate method, B3LYP/6-31G(d) level of theory.

The optimized geometry of *E*-SA shows that the side chain that bears the carboxylic unit deviates slightly from planarity, adopting a conformation that should favor the delocalization of the electron density in the anionic species (Fig. 6(a)). Thus, for the trihydrated complexes the largest deviation of the dihedral angle C2=C1—Cβ=Cα from planarity amounts to 23°, whereas the deviation of the carboxylic group is typically less than 5°. The inclusion of hydrating water molecules has little impact on the wavelength of absorption maxima. The results point out that protonation of the *E*-SA anionic species shifts the wavelength from 301 nm to 337 nm, whereas formation of the dianionic species shifts the absorption band to 371 nm (Table 2). Overall, these changes agree with the trends found in the experimental spectra shown in Fig. 5(c) and (d), which indicate the shifts from 313 nm (monoanionic) to 317 nm (neutral) and to 370 nm (dianion).

In contrast to *E*-SA, the side chain of *Z*-SA exhibits large deviations from planarity (Fig. 6(b)). Thus, the dihedral angle C2=C1—Cβ=Cα is close to 40° for both neutral and monoanionic (carboxylate) species, but such a deviation is largely diminished in the dianionic form. Likewise, significant deviations are also found for the carboxylic group, which are affected by the number of hydrating water molecules. For the trihydrated compounds, the wavelengths of the absorption maxima are predicted to change from 275 nm (monoanion, carboxylate) to 308 nm (neutral) and to 350 nm (dianion, carboxylate and phenolate), which reflect well the trends obtained for the pH-induced shifts (from 280 nm to 312 and 350 nm, respectively; see Fig. 5(a) and (b) and Table 2).

For both neutral *Z*- and *E*-SA, the most probable electronic transition is from the S_0 to the S_1 states, which presents oscillator strength of 0.25 and 0.64 for the *Z*- and *E*-SA, respectively. This transition corresponds to the transition from the highest occupied molecular orbital (HOMO) to the lowest unoccupied molecular orbital (LUMO). In the case of the mono anionic (carboxylate) species, *Z*- and *E*-SA$^-$, the most probable transition has also a minor contribution of the transition to the LUMO from HOMO-2 and HOMO-3 orbitals, respectively, in addition to the HOMO–LUMO transition. This excitation energy corresponds to the transition between the S_0 state, to the S_1 (oscillator strength 0.35) and S_2 (oscillator strength 0.54) excited states, for the mono anions *Z*- and *E*-SA$^-$, respectively.

4.4. Extension to other cinnamic acids

Other commercially available *E*-cinnamic acids were also checked, including *E*-3-hydroxy-4-methoxycinnamic acid (isomer ferulic acid, *E*-iFA), *E*-3,4-dihydroxycinnamic acid (*E*-caffeic acid, *E*-CAFA), *E*-4-nitrocinnamic acid (*E*-4NO2CA), *E*-4-aminocinnamic acid (*E*-4NH2CA), *E*-2-hydroxycinnamic acid (*E*-2OHCA), *E*-3-hydroxycinnamic acid (*E*-3OHCA), *E*-3-chloro-4-methoxycinnamic acid (*E*-3Cl4OMeCA) and 3-(*E*-3,4-dihydroxycinnamoyl)quinic acid (chlorogenic acid, 3-caffeoylquinic acid, *E*-CGA). All of them showed that the effect of acetonitrile, methanol and water on the UV absorption spectra is very minor (Figs. S8–S15 in Supplementary Material), which reflects the trends observed for *E*-FA and *E*-SA (data for *E*-CA, *E*-CUA and *E*-DMCA are also included in Supplementary Material, Figs. S2, S4 and S5).

Among these *E*-cinnamics, UV irradiation of caffeic acid (*E*-CAFA) solution for 7 h yielded a mixture of *Z*- and *E*-CAFA, thus reflecting the well known *E*- to *Z*-photoisomerization [29–32]. This result was supported by the comparison of the UV absorption spectra in methanol and in water solution (Fig. 7), and the formation of *Z*-CAFA was further confirmed by ^{1}H NMR (results not shown). This is an interesting application of UV absorption spectra in water for qualitative and quantitative determination of *Z*-cinnamic acids in natural samples containing mixture of both geometric isomers.

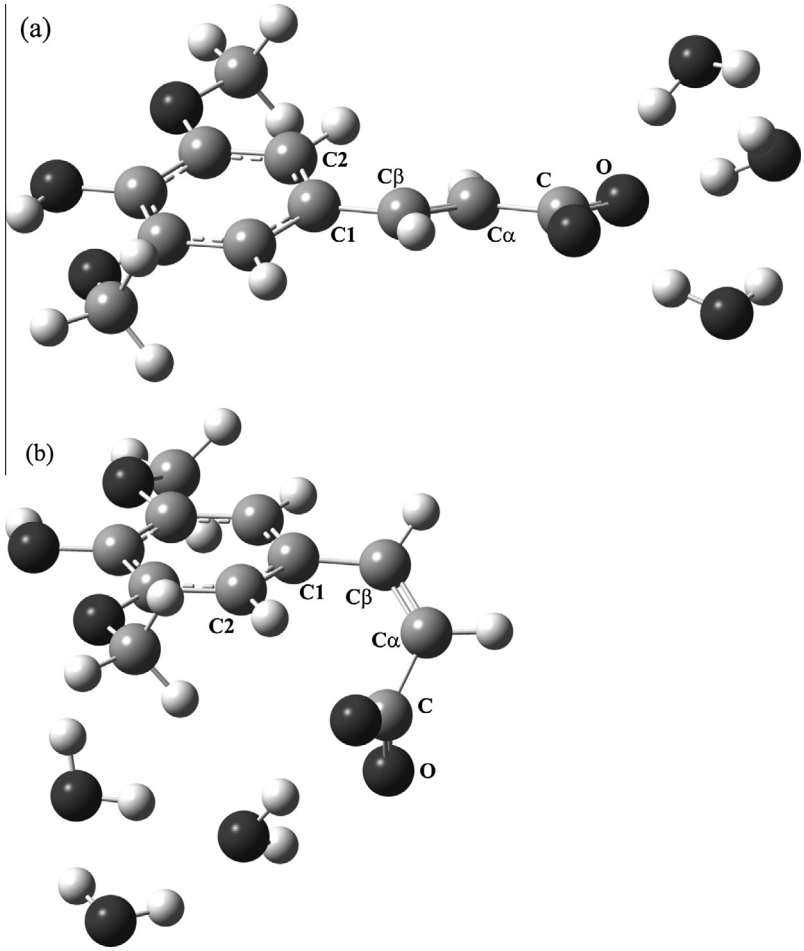

Fig. 6. Optimized structures of the three-hydrated mono anionic (carboxylate anion) species of (a) *E*- and (b) *Z*-SA at the MP2/6-311++G(d,p) level of theory. Labels of the atoms considered in dihedral angles are included.

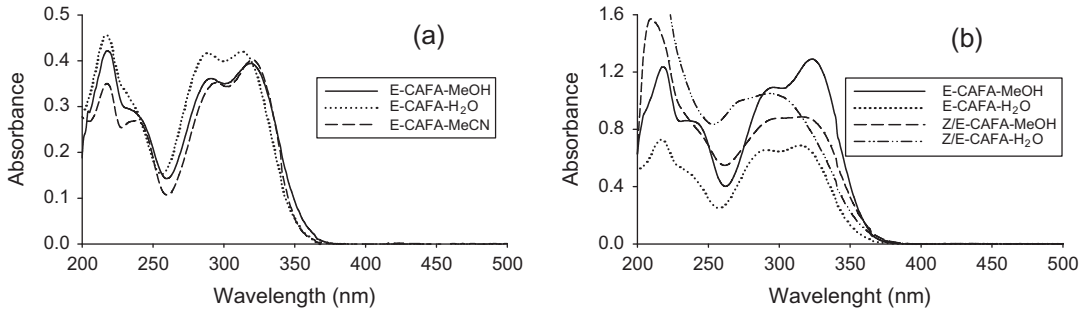

Fig. 7. Effect of solvent on the UV absorption spectra of (a) *E*-3,4-dihydroxycinnamic acid (*E*-CAFA). *E*-CAFA ($2.7 \cdot 10^{-5}$ M): --- MeCN, — MeOH, ··· H_2O; (b) *E*-CAFA ($2.7 \cdot 10^{-5}$ M): — MeOH, ··· H_2O; *E*-3,4-dihydroxycinnamic acid + Z-3,4-dihydroxycinnamic acid (*ZE*-CAFA), --- MeOH, -·-· H_2O.

5. Conclusions

A detailed description of the spectral properties of *Z*-cinnamic acids in water solution is presented in this study. The UV absorption spectra of several *Z*- and *E*-cinnamic acids reveal significant differences in the behavior of the two isomers. The results show a dramatic hypsochromic shift from methanolic to water solution for *Z*-cinnamic acids, while a minor blue shift is observed for the *E*-isomers. The pH experiments confirm the presence of neutral, monoanionic (carboxylate form) and dianionic species depending on the nature of the media, leading to different UV absorption spectra. Quantum chemical calculations show that in water solution the carboxylic side chain of deprotonated *Z*-cinnamic acids (carboxylate anionic form) adopt a twisted conformation, which alters the electronic density delocalization, in contrast with the planar structure found for *E*-cinnamic acids. The results give support to the use of UV absorption spectra as a powerful tool to characterize mixtures of cinnamic acids in aqueous media. Furthermore, the high-level quantum chemical calculations should be valuable to examine the functional and biotechnological roles of these compounds in condensed media.

Acknowledgements

The authors acknowledge the financial support from the National Research Council of Argentina (CONICET; PIP 0400), the

University of Buenos Aires (UBA X088 and X01/J080), the MINECO (SAF2011-27642), Generalitat de Catalunya (2014SGR1189) and XRQTC, and the CSUC for computational resources. FJL acknowledges the financial support from ICREA Academia. R.E-B, MLS and PAM are research members of CONICET (Argentina).

Appendix A. Supplementary material

Supplementary data associated with this article can be found, in the online version, at http://dx.doi.org/10.1016/j.jphotobiol.2015.03.032.

References

[1] L. Taiz, E. Zeiger, Plant Physiology, second ed., Sinauer Associated Inc., Pub, 1998.
[2] B.B. Buchanan, W. Gruissem, R.L. Jones, Biochemistry & Molecular Biology of Plants, Springer American Society of Plant Physiologist, Rockville, 2000, pp. 1286 (Chapter 24).
[3] F.A. Haskins, L.G. Williams, H.J. Gorz, Light-induced trans to cis conversión of β–D-glucosil-o-hydroxycinnamic acid in Melilotus alba leaves, Plant Physiol. 39 (1964) 777–781.
[4] J. Klepacka, L. Fornal, Ferulic acid and its position among the phenolic compounds of wheat, Crit. Rev. Food Sci. Nutr. 46 (2006) 639–647.
[5] R.A. Dixon, Natural products and plant disease resistance, Nature 411 (2001) 843–847.
[6] J.M. Humphreys, C. Chapple, Rewriting the lignin roadmap, Curr. Opin. Plant Biol. 5 (2002) 224–229.
[7] M. Sova, Antioxidant and antimicrobial activities of cinnamic acid derivatives, Mini Rev. Med. Chem. 12 (2012) 749–767.
[8] M.L. Salum, R. Erra-Balsells, High purity *cis*-cinnamic acid preparation for studying physiological role of *trans*-cinnamic and *cis*-cinnamic acids in higher plants (review), Environ. Control Biol. 52 (2013) 1–13.
[9] Z.Q. Yin, W.S. Wong, W.C. Ye, N. Li, Biologically active cis-cinnamic acid occurs naturally in *Brassica parachinensis*, Chin. Sci. Bull. 48 (2003) 555–558.
[10] W.S. Wong, D. Guo, X.L. Wang, Z.Q. Yin, B. Xia, N. Li, Study of *cis*-cinnamic acids in Arabidopsis thaliana, Plant Physiol. Biochem. 43 (2005) 929–937.
[11] D. Guo, W.S. Wong, W.Z. Xu, F.F. Sun, D.J. Qing, N. Li, *Cis-cinnamic acid-enhanced 1* gene plays a role in regulation of Arabidopsis bolting, Plant Mol. Biol. 75 (2011) 481–495.
[12] V.H. Salvador, R.B. Lima, W.D. dos Santos, A.R. Soares, P.A.F. Böhm, R. Marchiosi, M.L.L. Ferrarese, O. Ferrarese-Filho, Cinnamic acid increases and inhibits soybean root growth, PLOS One 8 (2013) e69105.
[13] M.L. Salum, C.J. Robles, R. Erra-Balsells, Photoisomerization of ionic liquids ammonium cinnamates: one-pot synthesis-isolation of Z-cinnamic acids, Org. Lett. 12 (2010) 4808–4811.
[14] M.L. Salum, R. Erra-Balsells, One-pot synthesis of Z-cinnamic acids. Argentine Patent, CONICET #20090105020, 2009.
[15] H.B. Schlegel, Optimization of equilibrium geometries and transition structures, J. Comput. Chem. 3 (1982) 214–218.
[16] H.B. Schlegel, Geometry optimization on potential energy surface, in: D.R. Yarkony (Ed.), Modern Electronic Structure Theory, World Scientific Publishing, Singapore, 1994.
[17] C. Adamo, V.J. Barone, Toward reliable density functionals without adjustable parameters: the PBE0 Model, J. Chem. Phys. 110 (1999) 6158–6170.
[18] T.H. Dunning Jr, Gaussian basis sets for use in correlated molecular calculations. I. The atoms boron through neon and hydrogen, J. Chem. Phys. 90 (1989) 1007–1023.
[19] J. Tomasi, B. Mennucci, R. Cammi, Quantum mechanical continuum solvation models, Chem. Rev. 105 (2005) 2999–3093.
[20] E. Cances, B. Mennucci, J. Tomasi, A new integral equation formalism for the polarizable continuum model: Theoretical background and applications to isotropic and anisotropic dielectrics, J. Chem. Phys. 107 (1997) 3032–3041.
[21] E. Cances, B. Mennucci, New applications of integral equation methods for solvation continuum models: ionic solutions and liquid crystals, J. Math. Chem. 23 (1998) 309–326.
[22] Gaussian 09, Revision A.02, M.J. Frisch, G.W. Trucks, H.B. Schlegel, G.E. Scuseria, M.A. Robb, J.R. Cheeseman, G. Scalmani, V. Barone, B. Mennucci, G.A. Petersson, H. Nakatsuji, M. Caricato, X. Li, H.P. Hratchian, A.F. Izmaylov, J. Bloino, G. Zheng, J.L. Sonnenberg, M. Hada, M. Ehara, K. Toyota, R. Fukuda, J. Hasegawa, M. Ishida, T. Nakajima, Y. Honda, O. Kitao, H. Nakai, T. Vreven, J.A. Montgomery, Jr., J.E. Peralta, F. Ogliaro, M. Bearpark, J.J. Heyd, E. Brothers, K.N. Kudin, V.N. Staroverov, R. Kobayashi, J. Normand, K. Raghavachari, A. Rendell, J.C. Burant, S.S. Iyengar, J. Tomasi, M. Cossi, N. Rega, J.M. Millam, M. Klene, J.E. Knox, J.B. Cross, V. Bakken, C. Adamo, J. Jaramillo, R. Gomperts, R.E. Stratmann, O. Yazyev, A.J. Austin, R. Cammi, C. Pomelli, J.W. Ochterski, R.L. Martin, K. Morokuma, V.G. Zakrzewski, G.A. Voth, P. Salvador, J.J. Dannenberg, S. Dapprich, A.D. Daniels, O. Farkas, J.B. Foresman, J.V. Ortiz, J. Cioslowski, D.J. Fox, Gaussian Inc, Wallingford CT, 2009.
[23] J.Z. Dávalos, R. Herreo, A. Chana, A. Guerrero, P. Jiménez, J.M. Santiuste, Energetics and structural properties, in the gas phase, of trans-hydroxycinnamic acids, J. Phys. Chem. A 116 (2012) 2261–2267.
[24] M.J. González Moa, M. Mandado, R.A. Mosquera, Charge density study of natural cinnamic acids, Chem. Phys. Lett. 424 (2006) 17–22.
[25] S.P. Ozkorucuklu, J.L. Beltrán, G. Fonrodona, D. Barrón, G. Alsancak, J. Barbosa, Determination of dissociation constants of some hydroxylated benzoic and cinnamic acids in water from mobility and spectroscopic data obtained by CE-DAD, J. Chem. Eng. Data 54 (2009) 807–811.
[26] C. Jamorski, M.E. Casida, D.R. Salahub, Dynamic polarizabilities and excitation spectra from a molecular implementation of time-dependent density-functional response theory: N_2 as a case study, J. Chem. Phys. 104 (1996) 5134–5147.
[27] M. Promkatkaew, S. Suramitr, T.M. Karpkird, S. Namuangruk, M. Ehara, S. Hannongbua, Absorption and emission spectra of ultraviolet B blocking methoxy substituted cinnamates investigated using the symmetry-adapted cluster configuration interaction method, J. Chem. Phys. 131 (224306) (2009) 1–10.
[28] M. Promkatkaew, S. Suramitr, T. Karpkird, M. Ehara, S. Hannongbua, Absorption and emission properties of various substituted cinnamic acids and cinnamates, based on TDDFT investigation, Int. J. Quantum Chem. 113 (2013) 542–554.
[29] T. Mori, Y. Inoue, C=C photoinduced isomerization reactions, in: A.G. Griesbeck, J. Mattay (Eds.), Synthetic Organic Photochemistry, Springer Marcel Dekker, New York, USA, 2005, pp. 417–452.
[30] N.J. Turro, V. Ramamurthy, J.C. Scaiano, Principles of Molecular Photochemistry: An Introduction, University Science Books, Sausalito, CA, 2009, p. 319.
[31] Y. Rao, R. Filler, Trans- to cis-isomerization of cinnamic acids and related carbonyl compounds, J. Chem. Soc., Chem. Commun. 12 (1976) 471–472.
[32] V.J. Rao, Photochemical cis-trans Isomerization from the Singlet State, in: V. Ramamurthy, K.S. Schanze (Eds.), Organic Molecular Photochemistry, vol. 3 in the Series, Molecular and Supramolecular Photochemistry, 1999, pp. 169.